Published in final edited form as:
*J Neurochem*. 2014 July ; 130(1): 87–96. doi:10.1111/jnc.12712.

# Proton-dependent zinc release from intracellular ligands

**Lech Kiedrowski**
The Psychiatric Institute, Departments of Psychiatry and Pharmacology, The University of Illinois at Chicago, Chicago, Illinois 60612, USA

## Abstract

In cultured cortical and hippocampal neurons when intracellular pH drops from 6.6 to 6.1, yet unclear intracellular stores release micromolar amounts of $Zn^{2+}$ into the cytosol. Mitochondria, acidic organelles, and/or intracellular ligands could release this $Zn^{2+}$. Although exposure to the protonophore FCCP precludes re-loading of the mitochondria and acidic organelles with $Zn^{2+}$, FCCP failed to compromise the ability of the intracellular stores to repeatedly release $Zn^{2+}$. Therefore, $Zn^{2+}$-releasing stores were not mitochondria or acidic organelles but rather intracellular $Zn^{2+}$ ligands. To test which ligands might be involved, the rate of acid-induced $Zn^{2+}$ release from complexes with cysteine, glutathione, histidine, aspartate, glutamate, glycine, and carnosine was investigated; [$Zn^{2+}$] was monitored *in vitro* using the ratiometric $Zn^{2+}$-sensitive fluorescent probe FuraZin-1. Carnosine failed to chelate $Zn^{2+}$ but did chelate $Cu^{2+}$; the remaining ligands chelated $Zn^{2+}$ and upon acidification were releasing it into the medium. However, when pH was decreasing from 6.6 to 6.1, only zinc-cysteine complexes rapidly accelerated the rate of $Zn^{2+}$ release. The zinc-cysteine complexes also released $Zn^{2+}$ when a histidine-modifying agent, diethylpyrocarbonate, was applied at pH 7.2. Since the cytosolic zinc-cysteine complexes can contain micromolar amounts of $Zn^{2+}$, these complexes may represent the stores responsible for an acid-induced intracellular $Zn^{2+}$ release.

### Keywords

FuraZin-1; Cysteine; Glutathione; Carnosine; Histidine; Diethylpyrocarbonate

## Introduction

Brain tissue acidifies shortly after the onset of ischemia (Siemkowicz and Hansen 1981; Smith et al. 1986) and acidosis is neurotoxic (Goldman et al. 1989; Nedergaard et al. 1991). The mechanisms of acid-induced cell death include the activation of acid-sensitive ion channels (Xiong et al. 2004; Wemmie et al. 2006), facilitation of apoptosis (Barry and Eastman 1992; Gottlieb et al. 1996), and an enhancement of oxidative damage (Siesjöet et

Correspondence to: Lech Kiedrowski, Ph.D., The Psychiatric Institute, 1601 W. Taylor St., Room 564, Chicago, IL 60612, Phone: 312 413-4559, Fax: 312 413-4569, lkiedr@psych.uic.edu.

Conflicts of interest
The author declares his involvement in SPOT culture kit production at the University of Illinois at Chicago Research Resources Center.
=> if 'none', insert "The authors have no conflict of interest to declare."
=> otherwise insert info unless it is already include

al. 1985; Ying et al. 1999). Recently, it has been demonstrated that acid-induced neuronal death is preceded by elevations of intracellular $[Zn^{2+}]$ ($[Zn^{2+}]_i$) (Isaev et al. 2010), which occur due to a $Zn^{2+}$ release from intracellular stores (Sensi et al. 2003; Kiedrowski 2011, 2012). Since an elevation of $[Zn^{2+}]_i$ compromises glycolysis (Ikeda et al. 1980; Krotkiewska and Banaś 1992) and mitochondrial function (Brown et al. 2000; Jiang et al. 2001), an acid-induced $[Zn^{2+}]_i$ elevation may become a target for stroke therapies. Therefore, the mechanism of acid-induced intracellular $Zn^{2+}$ release needs to be better understood. Although Sensi et al. (2003) suggested that $Zn^{2+}$ is released from mitochondria, it could also be released from acidic organelles that use the $H^+$ gradient to accumulate $Zn^{2+}$ (Colvin 2002; Ohana et al. 2009), or from metallothioneins which chelate $Zn^{2+}$, as suggested by Shuttleworth and Weiss (2011). Other yet unclear cytosolic $Zn^{2+}$ ligands might also play a role. The purpose of this work was to clarify the mechanisms responsible for intracellular $Zn^{2+}$ release in acidified neurons.

## Materials and Methods

### Primary cultures of mouse hippocampal and cortical neurons

Primary hippocampal and cortical cultures were prepared using SPOT™ kits from the University of Illinois at Chicago Research Resources Center (http://www.rrc.uic.edu/portal/SPOT_Culture_Kit). These kits contained brain tissue from c57/bl/6 mice at embryonic day 16. Kit production was approved by the Institutional Animal Care and Use Committee. Cultures were prepared as previously described (Kiedrowski, 2011) except that to improve long-term cell viability, glial proliferation was not prevented with cytostatic agents. Glial cells were identified after ion imaging experiments. To this end, the cells were fixed with 4% formaldehyde, exposed to a primary rabbit anti-GFAP (1:500, AB5804 Chemicon) antibody followed by a secondary TRITC-labeled goat anti-rabbit IgG (1:500, Sigma T6778), as described in Kiedrowski (2007). In many experiments, GFAP-positive cells could not be detected in the field that was being investigated (Fig. S1A and C). The cultures were used for experiments after two weeks *in vitro*.

### Experimental media

For fluorescence imaging, cultures were transferred to Locke's buffer containing (in mM) NaCl (157.6), KCl (2.0), $KHCO_3$ (3.6), $MgCl_2$ (1.0), $CaCl_2$ (1.3), glucose (5), and piperazine-1,4-bis(2-ethanesulfonic acid), PIPES (10); pH was adjusted to 7.2 or 6.1 using NaOH or HCl, respectively. To create $Ca^{2+}$-free and $Zn^{2+}$-free buffers, $CaCl_2$ was omitted and 100 μM EGTA was added.

### Fluorescence imaging and superfusion

Fluorescence imaging was performed using two instruments. Initially, an Attofluor digital imaging system (Atto Instruments, Rockville, MD) connected to a Zeiss Axiovert 100 microscope (Carl Zeiss Mikroskopie, Jena, Germany) was used, as described earlier (Kiedrowski 2011). More recently, a digital fluorescence imaging system controlled by MetaFluor 7.1 software, equipped with a Zeiss Axio Observer D1 microscope with a motorized dichroic turret, a 4-position Sutter excitation filter wheel, a 4-position Sutter emission filter wheel, a Sutter XL xenon illumination unit, a Sutter LAMBDA 10-3

controller, and a RETIGA EXi Blue camera (QImaging, Surrey, BC, Canada) was used. Fluorescence was monitored using a Zeiss Fluar 20×, NA 0.75 objective. Superfusion media were delivered directly onto the cells via an 8-channel manifold (MPRE-8, Cell MicroControls, Norfolk, VA); flow was computer-controlled using an 8-channel valve switch (cFlow8, Cell MicroControls). Cells were superfused at a rate of 0.5 ml/min. Temperature was maintained at 37 °C using a bipolar temperature controller (TC2BIP, Cell MicroControls).

### Simultaneous monitoring Fura2-FF and FluoZin-3 fluorescence

Cultures were loaded with Fura-2FF AM and FluoZin-3 AM and fluorescence was imaged in single cells as described in Kiedrowski (2012). Briefly, Fura-2FF data were collected as the ratio of fluorescence intensity measured after 340 and 380 nm excitations (F340/F380). FluoZin-3 data were collected as the fluorescence emitted after a 488 nm excitation (F488). At the end of the experiments, 20 μM 1-hydroxypyridine-2-thione zinc salt and 100 μM $ZnCl_2$ (ZnPyr) were applied to measure the Fura-2FF signal and the FluoZin-3 signal after saturation with $Zn^{2+}$ (Fig. S1 B). The Fura-2FF and FluoZin-3 data were expressed as a percentage of the respective ZnPyr signals.

### Monitoring intracellular pH ($pH_i$)

Cultures were loaded with 2′,7′-bis-(2-carboxyethyl)-5(6)-carboxyfluorescein acetoxymethyl ester (BCECF AM) and the fluorescence was monitored and calibrated as described in detail in Kiedrowski (2011).

### Simultaneous monitoring of mitochondrial membrane potential ($\Delta\psi m$) and Fura-2FF fluorescence

Cultures were loaded for 5 min at 37°C with 2 μM rhodamine 123 (Rh123) and 0.1 μM Fura-2FF AM. The Fura-2FF signal (F340/F380 ratio) was monitored as described above. Rh123 was excited at 488 nm and emissions over 520 nm were monitored. $\Delta\psi m$ was assessed in the Rh123 quenching mode. In this mode, mitochondrial depolarization is detected as an increase of Rh123 fluorescence intensity due to an unquenching of Rh123 released from the mitochondria to the cytosol (Perry et al. 2011). To measure the Rh123 signal associated with maximal depolarization, 3 μM carbonyl cyanide 4-(trifluoromethoxy)phenylhydrazone (FCCP) was applied to depolarize the mitochondria. Rh123 data were expressed as a percentage of the maximal signal.

### Measuring the affinity of FuraZin-1 for $Zn^{2+}$ at pH 7.2 and 6.1.

FuraZin-1 AM (1 mM in DMSO) was hydrolyzed with 1 M KOH, neutralized with 1 M HCl and diluted with $H_2O$ to obtain a 100 μM stock of FuraZin-1 potassium salt of which the aliquots were stored at −80 °C. The affinity of FuraZin-1 for $Zn^{2+}$ at pH 7.2 versus 6.1 was characterized using the PTI QuantaMaster spectrofluorometer (Birmingham, NJ). In these experiments, fluorescence excitation spectra (320 – 420 nm excitation, 490 nm emission) of 100 nM FuraZin-1 in a solution containing 100 mM KCl and 50 mM PIPES with pH 7.2 or 6.1 (adjusted with KOH) and $ZnCl_2$ ranging from 0.1 μM to 3 mM were measured at 37 °C. Continuous mixing was provided by a magnetic stirrer. The apparent FuraZin-1 $Zn^{2+}$

dissociation constants were calculated using SigmaPlot 10 software (Systat Software Inc., Richmond, CA) from the F340 and F340/F380 data.

### Assay of $Zn^{2+}$ release from ligands

Using the PTI QuantaMaster spectrofluorometer, the F340/F380 ratio was measured at 37 °C in a cuvette containing 100 mM KCl, 50 mM PIPES, 100 nM FuraZin-1, and 100 μM $ZnCl_2$, pH 7.2. Then 1 mM tested ligand (in some experiments 10 mM) was added to the cuvette and the F340/F380 ratios were measured while pH was gradually decreased (using 5 M HCl) until it reached 6.1; pH was monitored using a pH meter. To study $Zn^{2+}$ chelation at pH 7.1 - 7.9, 3-(N-morpholino)propanesulfonic acid, MOPS, was used as a pH buffer.

The effects of diethylpyrocarbonate, DEPC, on $Zn^{2+}$ chelation by cysteine were tested using the above described Metafluor 7.1-controlled imaging system. In these experiments, a custom-made imaging chamber filled with 200 nM FuraZin-1, 100 mM KCl, and 50 mM PIPES, pH 7.2, was placed in the LU-CB1 Leiden dish holder connected to the TC-102 temperature controller (Medical Systems Corp., Greenvale, NY) to maintain 37 °C. F340/380 ratios were measured during successive additions of 100 μM $ZnCl_2$, 100 μM cysteine, and 1 mM DEPC to the chamber. Mixing was provided by a custom-made device.

### Statistical analysis

The data were analyzed using the SigmaStat 3.5 software (Systat Software Inc., Richmond, CA). For multiple comparisons, ANOVA followed by the Newman-Student-Keuls test was used. The Student's t-test was used to compare data from two groups. The differences were considered statistically significant if they reached at least $p<0.05$.

### Reagents

Fura-2FF AM was obtained from Teflabs (Austin, TX, USA), FuraZin-1 AM from Molecular Probes (Eugene, OR), and BCECF AM, FluoZin-3 AM, rhodamine 123 from Invitrogen (Carlsbad, CA, USA). All other reagents were from Sigma-Aldrich (St Louis, MO, USA) unless stated otherwise.

## Results

The idea that mitochondria represent a major $Zn^{2+}$ store responsible for acid-induced $[Zn^{2+}]_i$ elevations (Sensi et al. 2003) was examined. The driving force for mitochondrial $Zn^{2+}$ accumulation is provided by the mitochondrial membrane potential ($\Delta\psi m$), which is compromised by protonophores such as FCCP. One may expect that as long as FCCP is present in the medium and depolarizes mitochondria, the latter cannot re-accumulate $Zn^{2+}$ (assuming that mitochondria released $Zn^{2+}$ when FCCP was applied). If mitochondria cannot re-accumulate $Zn^{2+}$, it must be assumed that they cannot re-release it either. This logic was tested in cultured cortical and hippocampal neurons continuously exposed to FCCP while an impact of repetitive pulses of the extracellular pH ($pH_o$) drop from 7.2 to 6.1 on $[Zn^{2+}]$ was investigated. To monitor $[Zn^{2+}]_i$, FluoZin-3, a $Zn^{2+}$-specific fluorescent probe (Zhao et al. 2009), was used. Since intracellular acidification may trigger a $Ca^{2+}$ release from intracellular stores (Ou-yang et al. 1994), $[Ca^{2+}]$ was also monitored. To

measure $[Ca^{2+}]_i$, Fura-2FF was used. As the excitation spectra of FluoZin-3 and Fura-2FF do not overlap, $[Zn^{2+}]_i$ and $[Ca^{2+}]_i$ could be monitored simultaneously. However, the Fura-2FF signal (F340/F380 ratio) increase may indicate a $[Ca^{2+}]_i$ or $[Zn^{2+}]_i$ elevation. To determine the extent to which the Fura-2FF signal reported $[Ca^{2+}]_i$, at the end of each experiment, a plasma-membrane permeable heavy metal chelator, 10 μM N,N,N′,N′-tetrakis(2-pyridylmethyl)ethylenediamine (TPEN), was applied. Such TPEN application obliterates the $[Zn^{2+}]_i$ increase without affecting $[Ca^{2+}]_i$ (Kiedrowski 2011). To ensure that the observed $[Zn^{2+}]_i$ or $[Ca^{2+}]_i$ elevations represented a $Zn^{2+}$ or $Ca^{2+}$ release from intracellular stores, the extracellular medium was free of $Zn^{2+}$ and $Ca^{2+}$.

In cortical and hippocampal neurons, upon application of 3 μM FCCP at pH 7.2, only a minor (less than 5%) increase of the FluoZin-3 signal was observed. However, in 6% of cortical (4 of 67) and 4% of hippocampal (9 of 229) neurons, the Fura-2FF signal rapidly increased to apparently probe-saturating levels (Fig. S1, neurons 1, 2). In the remaining neurons, the Fura-2FF signal behaved similar to the FluoZin-3 signal; as shown in Fig. 1a, both signals started to rapidly increase only after the $pH_o$ was lowered from 7.2 to 6.1. When the $pH_o$ was returned to 7.2, the signals decreased to their original levels. Triple repetitions of this maneuver resulted in three peaks in the FluoZin-3 and Fura-2FF signals in both cortical (Fig. 1a) and hippocampal neurons (Fig. S2). A statistical analysis of these peaks is shown in Fig. 1b. The three peaks of Fura-2FF signal, in cortical and hippocampal neurons, were progressively smaller, with the first peak by 84% and the second peak by 28% larger than the third peak (Fig. 1b, right). The three peaks of FluoZin-3 signals in cortical neurons were, however, approximately the same size, whereas in hippocampal neurons, the first peak was only about 16% larger ($p<0.05$) than the second peak and there was no statistically significant difference between the last two peaks (Fig. 1b, left). An application of 10 μM TPEN quenched the last peak of both FluoZin-3 and Fura-2FF signals to background levels. The data suggest that only $[Zn^{2+}]_i$ was responsible for FluoZin-3 and Fura-2FF signal elevation in the third peak whereas $[Ca^{2+}]_i$ elevation significantly contributed to the first peak.

Parallel experiments on neurons loaded with BCECF showed that when FCCP was applied at $pH_o$ 7.2, $pH_i$ decreased from 7.5 to about 7.0. When the $pH_o$ was adjusted to 6.1, the $pH_i$ dropped to 6.2. When the $pH_o$ was increased to 7.2, the $pH_i$ increased to 7.0, and so on (Fig. 1c). Together, the $[Zn^{2+}]_i$ and $pH_i$ data suggest that the $Zn^{2+}$ release from intracellular stores (Fig. 1a) was associated with a drop in $pH_i$. As the mitochondria in these neurons were constantly depolarized with FCCP, the $\Delta\psi m$ collapse *per se* played no role in the mechanism of $Zn^{2+}$ release.

The idea that FCCP causes intracellular $Zn^{2+}$ release because it depolarizes mitochondria was explored further; if this is the case, all agents that depolarize mitochondria should affect $[Zn^{2+}]_i$ the same way FCCP does. Mitochondria can be depolarized by an application of rotenone plus oligomycin (Rot/Oligo) (Budd and Nicholls 1996). In preliminary experiments performed on hippocampal neurons, it was established that after increasing the rotenone and oligomycin concentrations to 10 μM and 5 μg/ml, respectively, the rate of Rot/Oligo-induced $\Delta\psi m$ collapse approached that induced by an application of 3 μM FCCP. It was then tested how Rot/Oligo versus FCCP affects $[Zn^{2+}]_i$ and $\Delta\psi m$ at $pH_o$ 7.2 and 6.1. $\Delta\psi m$ was

monitored with Rh123, and $[Zn^{2+}]_i$ with Fura-2FF (using TPEN to chelate $Zn^{2+}$, it was established mostly $Zn^{2+}$ was responsible for the Fura-2FF signal increase). Since the excitation spectra of Rh123 and Fura-2FF do not overlap, $\Delta\psi m$ and $[Zn^{2+}]_i$ could be monitored simultaneously.

As shown in Fig. 2a, although an application of Rot/Oligo at $pH_o$ 7.2 promptly depolarized mitochondria, the rate of the Fura-2FF signal increase remained unchanged even after the $pH_o$ was decreased to 6.1. Parallel experiments on neurons loaded with BCECF showed that Rot/Oligo at $pH_o$ 6.1 caused only a small drop in $pH_i$ (to 6.7). When FCCP was applied after Rot/Oligo, an additional $pH_i$ drop was observed. This additional $pH_i$ drop coincided with an acceleration of the Fura-2FF signal increase. A large part of this signal increase was quenched by TPEN and therefore represented $[Zn^{2+}]_i$ rather than $[Ca^{2+}]_i$ elevations (Fig. 2a). These data again show that the $[Zn^{2+}]_i$ increase is associated with a $pH_i$ drop rather than a $\Delta\psi m$ collapse.

Fig. 2b shows another set of experiments in which FCCP was applied at $pH_o$ 7.2, similar to the application of Rot/Oligo in Fig. 2a. FCCP promptly depolarized mitochondria, as expected, and $pH_i$ stabilized at about 7.0. When the $pH_o$ was decreased to 6.1, the $pH_i$ gradually dropped below 6.6 and during this $pH_i$ decrease, an acceleration of the Fura-2FF signal increase took place. Again, after TPEN was applied to chelate $Zn^{2+}$, the Fura-2FF signal rapidly decreased (Fig. 2b).

Fig. 2c shows a statistical analysis of the Rh123, Fura-2FF, and $pH_i$ data at the time points indicated by the asterisks in Figs. 2 a and b. While both Rot/Oligo and FCCP depolarized mitochondria, the $pH_i$ drop and $[Zn^{2+}]_i$ elevation were significantly larger in the presence of FCCP than in the presence of Rot/Oligo. These data rule out the idea that FCCP causes an intracellular $Zn^{2+}$ release because it depolarizes mitochondria.

One may envision that acidic organelles that use $H^+$ gradient as the driving force to accumulate $Zn^{2+}$ (Colvin 2002; Ohana et al. 2009) could release $Zn^{2+}$ upon a drop in $pH_i$. However, these organelles cannot re-accumulate $Zn^{2+}$ after the $H^+$ gradient has collapsed. Since an application FCCP promptly dissipates $H^+$ gradients in all acidic organelles tested to date: lysosomes (Ohkuma et al. 1982), endosomes (Maranda et al. 2001), chromaffin granules (Cidon et al. 1983), and synaptic vesicles (Cidon and Sihra 1989), these organelles could not play major role in the repetitive acid-induced $[Zn^{2+}]_i$ elevations taking place in the presence of FCCP (Fig. 1a).

It has been suggested that acid-induced $[Zn^{2+}]_i$ elevations result from a $Zn^{2+}$ release from metallothioneins (Shuttleworth and Weiss 2011). However, pH drop alone (without coinciding oxidation) induces $Zn^{2+}$ release from metallothioneins only if pH drops below 5.0 (Jiang et al. 2000). In neurons, acid-induced intracellular $Zn^{2+}$ release takes place when the $pH_i$ drops from 6.6 to 6.1 (Fig. 1c); therefore, $Zn^{2+}$ might be released from ligands that bind $Zn^{2+}$ with a lower than metallothionein affinity. To identify such ligands, one could attempt to use $Zn^{2+}$-sensitive fluorescent probes. But a caveat is that when pH drops from 7.2 to 6.1, high affinity probes such as FluoZin-3 or Fura-2FF show about a10-fold decrease in their affinity for $Zn^{2+}$ (Kiedrowski 2012). Fortunately, this problem could be minimized

using a low affinity ratiometric $Zn^{2+}$ probe, FuraZin-1 (Gee et al. 2002); although acidification did affect FuraZin-1 fluorescence (Fig. S3 A-C), the plots of FuraZin-1 F340/F380 ratios as a function of [$Zn^{2+}$] at pH 7.2 and 6.1 nearly overlapped (Fig. S3 D). Therefore, FuraZin-1 could be used to study the impact of a pH drop on $Zn^{2+}$ release from various agents considered to be physiological $Zn^{2+}$ ligands: cysteine, histidine, glutathione (GSH), aspartate, glutamate, glycine, and carnosine (β-alanyl-L-histidine). Carnosine resides only in a subpopulation of olfactory neurons (Margolis 1974; Neidle and Kandera 1974) and in astrocytes (Biffo et al. 1990). The reason carnosine was tested is that this dipeptide contains a histidine whose amino group forms a peptide bond; this histidine binds $Zn^{2+}$ without the participation of the amino group, the same way the histidines in proteins do. Therefore, using carnosine, one can address the impact of pH on $Zn^{2+}$ binding by the histidines in proteins.

In these experiments after measuring the FuraZin-1 F340/F380 ratio at 100 μM [$Zn^{2+}$] and pH 7.2, 1 mM or 10 mM ligands were added to the cuvette to chelate $Zn^{2+}$. Depending on the affinity of the ligands for $Zn^{2+}$, a variable FuraZin-1 signal drop was observed. Then, to determine the impact of pH on the $Zn^{2+}$ chelation, the pH in the cuvette was manipulated by adding HCl or KOH.

All tested ligands with the exception of carnosine caused a drop in the FuraZin-1 signal indicating that the ligands chelated $Zn^{2+}$; when the pH was decreasing from 7.2 to 6.1, the ligands were releasing $Zn^{2+}$ (Fig. 3 a and b). However, a rapid acceleration of the rate of $Zn^{2+}$ release coinciding with a pH drop from 6.6 to 6.1 was only observed in the cysteine solution (Fig. 3a, inset).

The extent of the ligand-induced FuraZin-1 signal drop should be proportional to the ligand's affinity for $Zn^{2+}$ (log K). The respective log K values are as follows: cysteine, 9.11; GSH, 7.98; histidine, 6.51; aspartate, 5.87; glycine, 4.96; and glutamate, 4.72 (Martell et al. 2004). Unexpectedly, although GSH has a higher than histidine affinity for $Zn^{2+}$, at pH 7.2, 1 mM GSH chelated less $Zn^{2+}$ than 1 mM histidine (Fig. 3a). To clarify this inconsistency, the effect of pH in the 7.9 - 7.1 range on $Zn^{2+}$ binding by GSH was investigated. As shown in Fig. 3c, GSH started to lose its affinity for $Zn^{2+}$ at a pH as high as 7.7.

Interestingly, carnosine, an agent reported to chelate $Zn^{2+}$ (Corona et al. 2011), not only did not decrease, but consistently increased the FuraZin-1 F340/380 ratio by about 10% (Fig. 3a, arrow). These data indicate that carnosine did not chelate $Zn^{2+}$ but could chelate a contaminating ion that affected FuraZin-1 fluorescence. To test this possibility, the impact of EDTA (to chelate the contaminating ion) on the FuraZin-1 excitation spectra was examined. It was found that the addition of up to 200 nM EDTA boosted FuraZin-1 fluorescence. When more than 200 nM EDTA was applied, no further fluorescence intensity increase was observed (Fig. S4 A). This outcome indicates that the solution in which FuraZin-1 was dissolved (100 mM KCl and 50 mM PIPES) was contaminated with an ion that quenched FuraZin-1 fluorescence. As this ion was completely chelated by 200 nM EDTA, its concentration was not higher than 200 nM. To determine the identity of the contaminating ion, the impact of $Ca^{2+}$, $Mg^{2+}$, $Fe^{2+}$, and $Cu^{2+}$ on the FuraZin-1 excitation spectra was explored. It was found that only $Cu^{2+}$ quenched FuraZin-1 fluorescence (Fig. S4

B) and that this quenching was dose-dependently removed by carnosine (Fig. S4 C). These data indicate that carnosine is a potent $Cu^{2+}$ (but not $Zn^{2+}$) chelator.

The data in Fig. 3a show that the profile of the acid-induced $Zn^{2+}$ release from cysteine resembles that observed in acidified neurons in which there is a rapid acceleration of $[Zn^{2+}]_i$ increase (Fig. 1 a) at the time when the $pH_i$ drops below 6.6 (Fig. 1 c). Although these data indicate that, of the ligands tested, cysteine was the most likely source of $Zn^{2+}$, it has been suggested that histidine is the primary source of the acid-induced $[Zn^{2+}]_i$ elevations (McCranor et al. 2012). The importance of histidine as a source of $Zn^{2+}$ stems from the fact that an agent that covalently modifies the imidazole ring of histidine, diethylpyrocarbonate (DEPC), causes robust $[Zn^{2+}]_i$ elevations (Haase and Beyersmann 2002). However, DEPC is a highly reactive agent which might also affect the ability of cysteine to bind $Zn^{2+}$. To test whether this is the case, the impact of 1 mM DEPC on $Zn^{2+}$ chelation by 100 μM cysteine was investigated using FuraZin-1. As shown in Fig. 4, within five minutes after DEPC application, virtually all the $Zn^{2+}$ chelated by cysteine was released back into the medium.

## Discussion

This work addressed the mechanism of an acid-induced intracellular $Zn^{2+}$ release in neurons (Kiedrowski 2011, 2012). Although this release was promoted by FCCP, it did not coincide with the FCCP-induced $\Delta\psi m$ collapse but instead coincided with the FCCP-induced $pH_i$ drop below 6.6. Therefore, $Zn^{2+}$ release was triggered not by mitochondrial depolarization but by intracellular acidification. The latter resulted from the FCCP-mediated $H^+$ influx from the extracelluar medium into the cytosol. The driving force for this $H^+$ influx was provided by the pH gradient across the plasma membrane.

FCCP easily penetrates biological membranes; the FCCP-induced $H^+$ fluxes, by depolarizing mitochondria and dissipating $H^+$ gradients in acidic organelles, preclude $Zn^{2+}$ re-accumulation in acidic organelles and mitochondria. Since FCCP failed to compromise the ability of the intracellular stores to repeatedly release $Zn^{2+}$, the $Zn^{2+}$-releasing stores were neither mitochondria nor acidic organelles but rather intracellular $Zn^{2+}$ ligands. When the pH was decreasing from 6.6 to 6.1, only the zinc-cysteine complexes showed a rapid acceleration in the rate of $Zn^{2+}$ release (Fig. 3a). Therefore, the acid-induced $[Zn^{2+}]_i$ elevations that took place in a similar range of the $pH_i$ drop (Fig. 1a) most likely resulted from a $Zn^{2+}$ release from the cytosolic zinc-cysteine complexes.

In the cytosol, cysteine-bound $Zn^{2+}$ exists in three fractions: large molecular weight proteins (proteome), 10kDa proteins (metallothioneins), and low molecular weight ligands (Nowakowski and Petering 2012). Since metallothioneins are not likely to release $Zn^{2+}$ when the pH drops from 6.6 to 6.1, $Zn^{2+}$ must be released from the proteomic or low molecular weight fraction or from both. The low molecular weight fraction contains molecules with an average molecular weight slightly larger than GSH, probably ZnGSH (Rana et al. 2008). Since the rate of $Zn^{2+}$ release from ZnGSH does not accelerate when pH drops from 6.6 to 6.1 (Fig. 3a), $Zn^{2+}$ is probably released from proteomic cysteines.

The proteomic cysteines not involved in disulphide bonds are able to chelate $Zn^{2+}$ and 21% of these cysteines reside in the evolutionally preserved CXXC motifs where X can be any coded amino acid (Miseta and Csutora 2000). Two CXXC motifs are often spatially arranged to form a zinc finger in which four cysteines coordinate one $Zn^{2+}$ (Ye et al. 2007). In such tetrahedral complexes, $Zn^{2+}$ is bound very tightly and probably does not dissociate at pH 6.1 (similar to the $Zn^{2+}$ in metallothioneins).

EGTA, is able to chelate 32% of proteomic $Zn^{2+}$ (Rana et al. 2008). The $Zn^{2+}$ log K value of EGTA is 12.6. Therefore, EGTA may remove $Zn^{2+}$ from the complexes in which one cysteine chelates one $Zn^{2+}$, ZnCys (log K = 9.1) (Martell et al. 2004). Acidification destabilizes the ZnCys complexes. The log K value of ZnHCys complexes is only 4.6 (Martell et al. 2004); in these complexes, $Zn^{2+}$ is bound so weakly that probes such as FluoZin-3 or Fura-2FF with affinity for $Zn^{2+}$ in the nanomolar range may strip it. When pH drops below 6.5, $Zn^{2+}$ dissociates from these complexes (Perrin and Sayce 1968).

A previous study performed on hippocampal neurons exposed to $pH_o$ 6.0 in the presence of gramicidin (to facilitate proton influx) addressed the amount of $Zn^{2+}$ released from intracellular $Zn^{2+}$ stores; it was estimated that about 1.3 μM $Zn^{2+}$ was released (Kiedrowski 2012). If this $Zn^{2+}$ had been released primarily from ZnCys complexes and considering that these complexes had released about 80% of $Zn^{2+}$ (Fig. 3a), the concentration of the ZnCys complexes prior to acidification would have to be 1.3 μM/0.8 = 1.6 μM. To approximate the amount of cysteine needed to form 1.6 μM ZnCys complex, a classic steady-state equilibrium binding equation can be used:

$$[ZnCys] = \left[Cys_{\mathrm{T}}\right] \times [Zn] / (\mathrm{K_d} + [Zn]) \quad (1)$$

where $K_d$ is the dissociation constant, [Zn] is the concentration of free $Zn^{2+}$, and [$Cys_T$] is the total concentration of cysteine. After rearranging equation (1) to:

$$\left[Cys_{\mathrm{T}}\right] = [ZnCys] \times (\mathrm{K_d} + [Zn]) / [Zn] \quad (2)$$

and entering 1.6 μM for [ZnCys], 0.000776 μM for $K_d$ (this corresponds to log K = 9.11), and 0.0006 μM for the basal [$Zn^{2+}$] (Krężel and Maret 2006), [$Cys_T$] = 3.6 μM. This means that when 3.6 μM cysteine and 0.0006 μM $Zn^{2+}$ are in equilibrium, the concentration of ZnCys complex is about 1.6 μM. However, the $K_d$ value used in equation (2) does not apply to all cytosolic cysteines because the affinity of proteomic cysteines for $Zn^{2+}$ may vary depending on a local environment and pH. Therefore, the result indicating that 3.6 μM cysteine can bind 1.6 μM $Zn^{2+}$ may not accurately reflect the amount of $Zn^{2+}$ chelated in all cytosolic ZnCys complexes.

Nevertheless, in the cytosol, there is much more than 3.6 μM cysteine available for $Zn^{2+}$ chelation; the concentration of free cysteine alone is 80 – 140 μM (Anderson and Meister 1989). Therefore there must be much more than 1.6 μM $Zn^{2+}$ chelated in ZnCys complexes, and upon acidification much more than the previously estimated 1.3 μM $Zn^{2+}$ (Kiedrowski 2012) must be released. A likely reason that the released $Zn^{2+}$ escaped detection is that most of it was intercepted by various cytosolic buffers that at pH close to 6 could chelate $Zn^{2+}$,

for example by metallothioneins. Considering that metallothioneins themselves release $Zn^{2+}$ when exposed to oxidants (Malaiyandi et al. 2004) or nitric oxide (St Croix et al. 2002), it is possible that if oxidative and/or nitrosative stress coincides with intracellular acidosis, which happens during ischemia/reperfusion, a mild oxidative/nitrosative stimulus normally insufficient to induce $Zn^{2+}$ release from metallothioneins could be sufficient under such conditions. Further research is necessary to clarify these possibilities.

Using equation 2, it has been calculated that 3.6 μM cysteine could chelate 1.6 μM $Zn^{2+}$; when analogous calculations are performed for other ligands, it can be found that 29.5 μM GSH, 825 μM histidine, 3.6 mM aspartate, 29.2 mM glycine, or 50.8 mM glutamate is necessary to chelate 1.6 μM $Zn^{2+}$. One may notice, that of all of these ligands, only the intracellular GSH concentration, 2.5 – 15 mM (Rice and Russo-Menna 1998; Mari et al. 2009), is high enough to chelate this much and even more $Zn^{2+}$. However, GSH chelated $Zn^{2+}$ well only when the pH was close to 8 (Fig. 3c). Considering that 8 is the pH of the mitochondrial matrix (Llopis et al. 1998) and that this matrix contains large amounts of GSH (Mari et al. 2009), GSH may play a more important role in $Zn^{2+}$ chelation in the mitochondrial matrix than in the cytosol. One may envision the following scenario: when the mitochondrial matrix pH drops from 8 to 7, GSH starts to release $Zn^{2+}$ (Fig. 3c) and this released $Zn^{2+}$ leaks into the cytosol; at pH 7 ligands such as metallothioneins and cysteine intercept the released $Zn^{2+}$; only after the pH drops below 6.6 and cysteine loses its affinity for $Zn^{2+}$, does $[Zn^{2+}]_i$ elevation become evident. This way, the $Zn^{2+}$ released from the mitochondrial GSH could contribute to acid-induced $[Zn^{2+}]$ elevations in the cytosol.

The idea that intracellular acidification may affect $[Ca^{2+}]_i$ was addressed in several previous studies with the conclusion that a $pH_i$ drop can trigger a $Ca^{2+}$ release from intracellular stores. Some of these studies were conducted using Fura-2 (Ou-yang et al. 1994), which responds to $Ca^{2+}$ and $Zn^{2+}$ (Grynkiewicz et al. 1985). Therefore, it is not clear to what extent $[Ca^{2+}]$ versus $[Zn^{2+}]_i$ elevations affected the Fura-2 signal. Nevertheless, in snail neurons, acid-induced $[Ca^{2+}]_i$ elevations were detected using $Ca^{2+}$-sensitive microelectrodes (Thomas 2002). The present data confirm that intracellular acidification can trigger $Ca^{2+}$ release from an internal store. In contrast to the store that releases $Zn^{2+}$, the store that releases $Ca^{2+}$ becomes depleted during repeated exposures to a low pH. Most likely this is because the released $Ca^{2+}$ is extruded to the extracellular medium more efficiently than $Zn^{2+}$.

As shown in Fig. 3a, carnosine failed to chelate $Zn^{2+}$ in an assay in which even the weak $Zn^{2+}$ chelators, glutamate and glycine, were effective. This result is consistent with the fact that carnosine has a lower than glutamate or glycine affinity for $Zn^{2+}$, log K= 4.0 (Martell et al. 2004). Most likely, single proteomic histidines, similar to carnosine, bind $Zn^{2+}$ poorly. Whereas in many proteins histidines are involved in $Zn^{2+}$ coordination (Vallee and Falchuk 1993), the latter is always mediated simultaneously by several histidines (or other amino acids) and such $Zn^{2+}$ binding is tight and resists acidification. For example, in a zinc metalloenzyme, alkaline phosphatase, a pH drop to 4.9 does not affect $Zn^{2+}$ coordination by histidines (Gettins and Coleman 1983).

The idea that histidine is a major $Zn^{2+}$-releasing ligand comes from the fact that the DEPC-mediated modification of imidazole is associated with an intracellular $Zn^{2+}$ release (Haase and Beyersmann 2002). Since DEPC also promoted a $Zn^{2+}$ release from cysteine (Fig. 4), the DEPC-induced $[Zn^{2+}]_i$ elevations most likely result from a DEPC-mediated $Zn^{2+}$ release from zinc-cysteine complexes.

That large amounts of $Zn^{2+}$ are stored in zinc-cysteine complexes is indicated by the fact that an application of a sulfhydryl reactive agent, N-ethylmaleimide, leads to a major intracellular $Zn^{2+}$ release (Haase and Beyersmann 2002; Nowakowski and Petering 2012). Interestingly, the released $Zn^{2+}$ was shown to accumulate in $Zn^{2+}$-storing organelles, which prior to the N-ethylmaleimide application contained only small amounts of labile $Zn^{2+}$ (Haase and Beyersmann 2002). If such organelles are not loaded with large amounts of $Zn^{2+}$ under basal conditions, they are not likely to play a major role in an acid-induced intracellular $Zn^{2+}$ release. This observation supports the general conclusion of the present report that acid-induced $[Zn^{2+}]$ elevations are caused by a $Zn^{2+}{}_i$ release from cytosolic zinc-cysteine complexes.

## Supplementary Material

Refer to Web version on PubMed Central for supplementary material.

## Acknowledgments

This work was supported by National Institutes of Health Grants 1R03NS077095 and 1R21NS082786 and a part of the work was presented on poster 350.04 at the 2012 Society for Neuroscience Meeting. The author is grateful to Drs. Peter Gettins, Thomas O'Halloran, and C. William Shuttleworth for inspiring discussions on the subject and additionally to Dr. Gettins for access to the PTI QuantaMaster spectrofluorometer. The author declares his involvement in SPOT™ culture kit production at the University of Illinois at Chicago Research Resources Center.

## Abbreviations used

| | |
|---|---|
| **BCECF** | 2′,7′-bis-(2-carboxyethyl)-5(6)-carboxyfluorescein |
| **$[Ca^{2+}]_i$ and $[Zn^{2+}]_i$** | intracellular $Ca^{2+}$ and $Zn^{2+}{}_i$ concentration |
| **DEPC** | diethylpyrocarbonate |
| **FCCP** | carbonyl cyanide 4-(trifluoromethoxy)phenylhydrazone |
| **GSH** | glutathione |
| **$pH_i$ and $pH_o$** | intracellular and extracellular pH |
| **ZnPyr signal** | Fura-2FF or FluoZin-3 signal after application of zinc + pyrithione |
| **MOPS** | 3-(N-morpholino)propanesulfonic acid |
| **PIPES** | piperazine-1,4-bis(2-ethanesulfonic acid) |
| **Rh123** | rhodamine 123 |
| **TPEN** | N,N,N′,N′-tetrakis(2-pyridylmethyl)ethylenediamine |

## References


Anderson ME, Meister A. Marked increase of cysteine levels in many regions of the brain after administration of 2-oxothiazolidine-4-carboxylate. FASEB J. 1989; 3:1632–1636. [PubMed: 2920877]

Barry MA, Eastman A. Endonuclease activation during apoptosis: the role of cytosolic $Ca^{2+}$ and pH. Biochem. Biophys. Res. Commun. 1992; 186:782–789. [PubMed: 1323291]

Biffo S, Grillo M, Margolis FL. Cellular localization of carnosine-like and anserine-like immunoreactivities in rodent and avian central nervous system. Neuroscience. 1990; 35:637–651. [PubMed: 2199844]

Brown AM, Kristal BS, Effron MS, Shestopalov AI, Ullucci PA, Sheu KF, Blass JP, Cooper AJ. $Zn^{2+}$ inhibits alpha-ketoglutarate-stimulated mitochondrial respiration and the isolated alpha-ketoglutarate dehydrogenase complex. J. Biol. Chem. 2000; 275:13441–13447. [PubMed: 10788456]

Budd SL, Nicholls DG. A reevaluation of the role of mitochondria in neuronal $Ca^{2+}$ homeostasis. J. Neurochem. 1996; 66:403–411. [PubMed: 8522981]

Cidon S, Ben-David H, Nelson N. ATP-driven proton fluxes across membranes of secretory organelles. J. Biol. Chem. 1983; 258:11684–11688. [PubMed: 6619137]

Cidon S, Sihra TS. Characterization of a H+-ATPase in rat brain synaptic vesicles. Coupling to L-glutamate transport. J. Biol. Chem. 1989; 264:8281–8288. [PubMed: 2566604]

Colvin RA. pH dependence and compartmentalization of zinc transported across plasma membrane of rat cortical neurons. Am. J. Physiol. Cell Physiol. 2002; 282:C317–329. [PubMed: 11788343]

Corona C, Frazzini V, Silvestri E, Lattanzio R, La Sorda R, Piantelli M, Canzoniero LM, Ciavardelli D, Rizzarelli E, Sensi SL. Effects of dietary supplementation of carnosine on mitochondrial dysfunction, amyloid pathology, and cognitive deficits in 3xTg-AD mice. PLoS One. 2011; 6:e17971. [PubMed: 21423579]

Gee KR, Zhou ZL, Ton-That D, Sensi SL, Weiss JH. Measuring zinc in living cells. A new generation of sensitive and selective fluorescent probes. Cell Calcium. 2002; 31:245–251. [PubMed: 12098227]

Gettins P, Coleman JE. 31P nuclear magnetic resonance of phosphoenzyme intermediates of alkaline phosphatase. J. Biol. Chem. 1983; 258:408–416. [PubMed: 6336753]

Goldman SA, Pulsinelli WA, Clarke WY, Kraig RP, Plum F. The effects of extracellular acidosis on neurons and glia in vitro. J. Cereb. Blood Flow Metab. 1989; 9:471–477. [PubMed: 2738113]

Gottlieb RA, Nordberg J, Skowronski E, Babior BM. Apoptosis induced in Jurkat cells by several agents is preceded by intracellular acidification. Proc. Natl. Acad. Sci. USA. 1996; 93:654–658. [PubMed: 8570610]

Grynkiewicz G, Poenie M, Tsien RY. A new generation of $Ca^{2+}$ indicators with greatly improved fluorescence properties. J. Biol. Chem. 1985; 260:3440–3450. [PubMed: 3838314]

Haase H, Beyersmann D. Intracellular zinc distribution and transport in C6 rat glioma cells. Biochem. Biophys. Res. Commun. 2002; 296:923–928. [PubMed: 12200136]

Ikeda T, Kimura K, Morioka S, Tamaki N. Inhibitory effects of $Zn^{2+}$ on muscle glycolysis and their reversal by histidine. J. Nutr. Sci. Vitaminol. (Tokyo). 1980; 26:357–366. [PubMed: 6453212]

Isaev NK, Stelmashook EV, Lukin SV, Freyer D, Mergenthaler P, Zorov DB. Acidosis-induced zinc-dependent death of cultured cerebellar granule neurons. Cell. Mol. Neurobiol. 2010; 30:877–883. [PubMed: 20373017]

Jiang D, Sullivan PG, Sensi SL, Steward O, Weiss JH. $Zn^{2+}$ induces permeability transition pore opening and release of pro-apoptotic peptides from neuronal mitochondria. J. Biol. Chem. 2001; 276:47524–47529. [PubMed: 11595748]

Jiang LJ, Vasak M, Vallee BL, Maret W. Zinc transfer potentials of the alpha - and beta-clusters of metallothionein are affected by domain interactions in the whole molecule. Proc. Natl. Acad. Sci. U S A. 2000; 97:2503–2508. [PubMed: 10716985]

Kiedrowski L. Critical role of sodium in cytosolic [$Ca^{2+}$] elevations in cultured hippocampal CA1 neurons during anoxic depolarization. J. Neurochem. 2007; 100:915–923. [PubMed: 17241128]

Kiedrowski L. Cytosolic zinc release and clearance in hippocampal neurons exposed to glutamate - the role of pH and sodium. J. Neurochem. 2011; 117:231–243. [PubMed: 21255017]

Kiedrowski L. Cytosolic acidification and intracellular zinc release in hippocampal neurons. J. Neurochem. 2012; 121:438–450. [PubMed: 22339672]

Krężel A, Maret W. Zinc-buffering capacity of a eukaryotic cell at physiological pZn. J. Biol. Inorg. Chem. 2006; 11:1049–1062. [PubMed: 16924557]

Krotkiewska B, Banaś T. Interaction of $Zn^{2+}$ and $Cu^{2+}$ ions with glyceraldehyde-3-phosphate dehydrogenase from bovine heart and rabbit muscle. Int. J. Biochem. 1992; 24:1501–1505. [PubMed: 1426532]

Llopis J, McCaffery JM, Miyawaki A, Farquhar MG, Tsien RY. Measurement of cytosolic, mitochondrial, and Golgi pH in single living cells with green fluorescent proteins. Proc. Natl. Acad. Sci. USA. 1998; 95:6803–6808. [PubMed: 9618493]

Malaiyandi LM, Dineley KE, Reynolds IJ. Divergent consequences arise from metallothionein overexpression in astrocytes: zinc buffering and oxidant-induced zinc release. Glia. 2004; 45:346–353. [PubMed: 14966866]

Maranda B, Brown D, Bourgoin S, Casanova JE, Vinay P, Ausiello DA, Marshansky V. Intra-endosomal pH-sensitive recruitment of the Arf-nucleotide exchange factor ARNO and Arf6 from cytoplasm to proximal tubule endosomes. J. Biol. Chem. 2001; 276:18540–18550. [PubMed: 11278939]

Margolis FL. Carnosine in the primary olfactory pathway. Science. 1974; 184:909–911. [PubMed: 4825893]

Mari M, Morales A, Colell A, Garcia-Ruiz C, Fernandez-Checa JC. Mitochondrial glutathione, a key survival antioxidant. Antioxid. Redox Signal. 2009; 11:2685–2700. [PubMed: 19558212]

Martell AE, Smith RM, Motekaitis RJ. NIST Critically Selected Stability Constants of Metal Complexes. NIST Standard Reference Database 46 Version 8. 2004

McCranor BJ, Bozym RA, Vitolo MI, Fierke CA, Bambrick L, Polster BM, Fiskum G, Thompson RB. Quantitative imaging of mitochondrial and cytosolic free zinc levels in an in vitro model of ischemia/reperfusion. J. Bioenerg. Biomembr. 2012; 44:253–263. [PubMed: 22430627]

Miseta A, Csutora P. Relationship between the occurrence of cysteine in proteins and the complexity of organisms. Mol Biol Evol. 2000; 17:1232–1239. [PubMed: 10908643]

Nedergaard M, Goldman SA, Desai S, Pulsinelli WA. Acid-Induced death in neurons and glia. J. Neurosci. 1991; 11:2489–2497. [PubMed: 1869926]

Neidle A, Kandera J. Carnosine - an olfactory bulb peptide. Brain Res. 1974; 80:359–364. [PubMed: 4423212]

Nowakowski A, Petering D. Sensor specific imaging of proteomic $Zn^{2+}$ with zinquin and TSQ after cellular exposure to N-ethylmaleimide. Metallomics. 2012; 4:448–456. [PubMed: 22498931]

Ohana E, Hoch E, Keasar C, Kambe T, Yifrach O, Hershfinkel M, Sekler I. Identification of the $Zn^{2+}$ binding site and mode of operation of a mammalian $Zn^{2+}$ transporter. J. Biol. Chem. 2009; 284:17677–17686. [PubMed: 19366695]

Ohkuma S, Moriyama Y, Takano T. Identification and characterization of a proton pump on lysosomes by fluorescein-isothiocyanate-dextran fluorescence. Proc. Natl. Acad. Sci. U S A. 1982; 79:2758–2762. [PubMed: 6178109]

Ou-yang YB, Mellergård P, Kristián T, Kristánova V, Siesjö BK. Influence of acid-base changes on the intracellular calcium concentration of neurons in primary culture. Exp. Brain Res. 1994; 101:265–271. [PubMed: 7843312]

Perrin DD, Sayce IG. Complex formation by nickel and zinc with penicillamine and cysteine. J. Chem. Soc. (A). 1968:53–57.

Perry SW, Norman JP, Barbieri J, Brown EB, Gelbard HA. Mitochondrial membrane potential probes and the proton gradient: a practical usage guide. Biotechniques. 2011; 50:98–115. [PubMed: 21486251]

Rana U, Kothinti R, Meeusen J, Tabatabai NM, Krezoski S, Petering DH. Zinc binding ligands and cellular zinc trafficking: apo-metallothionein, glutathione, TPEN, proteomic zinc, and Zn-Sp1. J. Inorg. Biochem. 2008; 102:489–499. [PubMed: 18171589]

Rice ME, Russo-Menna I. Differential compartmentalization of brain ascorbate and glutathione between neurons and glia. Neuroscience. 1998; 82:1213–1223. [PubMed: 9466441]

Sensi SL, Ton-That D, Sullivan PG, Jonas EA, Gee KR, Kaczmarek LK, Weiss JH. Modulation of mitochondrial function by endogenous $Zn^{2+}$ pools. Proc. Natl. Acad. Sci. U S A. 2003; 100:6157–6162. [PubMed: 12724524]

Shuttleworth CW, Weiss JH. Zinc: new clues to diverse roles in brain ischemia. Trends Pharmacol. Sci. 2011; 32:480–486. [PubMed: 21621864]

Siemkowicz E, Hansen AJ. Brain extracellular ion composition and EEG activity following 10 minutes ischemia in normo- and hyperglycemic rats. Stroke. 1981; 12:236–240. [PubMed: 7233472]

Siesjö BK, Bendek G, Koide T, Westerberg E, Wieloch T. Influence of acidosis on lipid peroxidation in brain tissues in vitro. J. Cereb. Blood Flow Metab. 1985; 5:253–258. [PubMed: 3988824]

Smith ML, von Hanwehr R, Siesjö BK. Changes in extra- and intracellular pH in the brain during and following ischemia in hyperglycemic and in moderately hypoglycemic rats. J. Cereb. Blood Flow Metab. 1986; 6:574–583. [PubMed: 3760041]

St Croix CM, Wasserloos KJ, Dineley KE, Reynolds IJ, Levitan ES, Pitt BR. Nitric oxide-induced changes in intracellular zinc homeostasis are mediated by metallothionein/thionein. Am. J. Physiol. Lung Cell. Mol. Physiol. 2002; 282:L185–192. [PubMed: 11792622]

Thomas RC. The effects of HCl and $CaCl_2$ injections on intracellular calcium and pH in voltage-clamped snail (Helix aspersa) neurons. J. Gen. Physiol. 2002; 120:567–579. [PubMed: 12356857]

Vallee BL, Falchuk KH. The biochemical basis of zinc physiology. Physiol. Rev. 1993; 73:79–118. [PubMed: 8419966]

Wemmie JA, Price MP, Welsh MJ. Acid-sensing ion channels: advances, questions and therapeutic opportunities. Trends Neurosci. 2006; 29:578–586. [PubMed: 16891000]

Xiong ZG, Zhu XM, Chu XP, Minami M, Hey J, Wei WL, MacDonald JF, Wemmie JA, Price MP, Welsh MJ, Simon RP. Neuroprotection in ischemia: blocking calcium-permeable acid-sensing ion channels. Cell. 2004; 118:687–698. [PubMed: 15369669]

Ye J, Cho SH, Fuselier J, Li W, Beckwith J, Rapoport TA. Crystal structure of an unusual thioredoxin protein with a zinc finger domain. J. Biol. Chem. 2007; 282:34945–34951. [PubMed: 17913712]

Ying W, Han SK, Miller JW, Swanson RA. Acidosis potentiates oxidative neuronal death by multiple mechanisms. J. Neurochem. 1999; 73:1549–1556. [PubMed: 10501200]

Zhao J, Bertoglio BA, Devinney MJ Jr. Dineley KE, Kay AR. The interaction of biological and noxious transition metals with the zinc probes FluoZin-3 and Newport Green. Anal. Biochem. 2009; 384:34–41. [PubMed: 18848515]

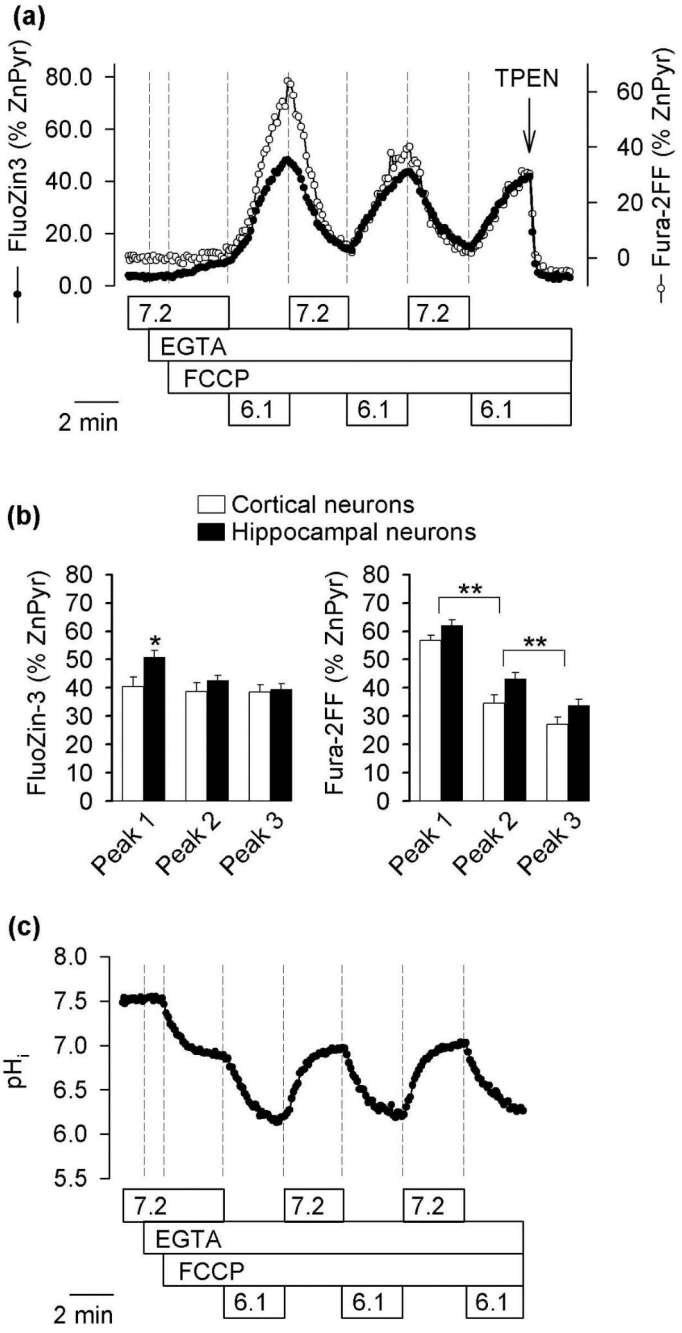


**Fig. 1.**

Effects of repetitive applications of low pH on $[Zn^{2+}]_i$, $[Ca^{2+}]_i$, and $pH_i$ in neurons. (a) Effects of repetitive acidifications on FluoZin-3 and Fura-2FF signals in cortical neurons. Indicated in the legend are: $pH_o$ (7.2 or 6.1), superfusion with $Ca^{2+}$- free and $Zn^{2+}$-free medium (EGTA), and applications of 3 μM FCCP and 10 μM TPEN. The data are percentages of FluoZin-3 and Fura-2FF signals measured after an application of 100 μM $ZnCl_2$ plus 10 μM pyrithione (ZnPyr) to saturate the probes with $Zn^{2+}$ (for details see Methods). The plots are scaled such that the third peak of Fura-2FF signal overlaps the

FluoZin-3 signal. The data are means (12 neurons) from a single experiment that was repeated five times with similar results. (b) Average peaks of FluoZin-3 and Fura-2FF signals in cortical and hippocampal neurons from experiments analogous to that shown in (a). The data are means ± SEM from five experiments on cortical neurons and six experiments on hippocampal neurons; ** $p < 0.01$, * $p < 0.05$, one-way ANOVA followed by Student-Newman-Keuls test. (c) Effects of repetitive acidifications on $pH_i$ in cortical neurons. The data are means (14 neurons) from a single experiment that was repeated three times with similar results. The experimental conditions are the same as described in (a).

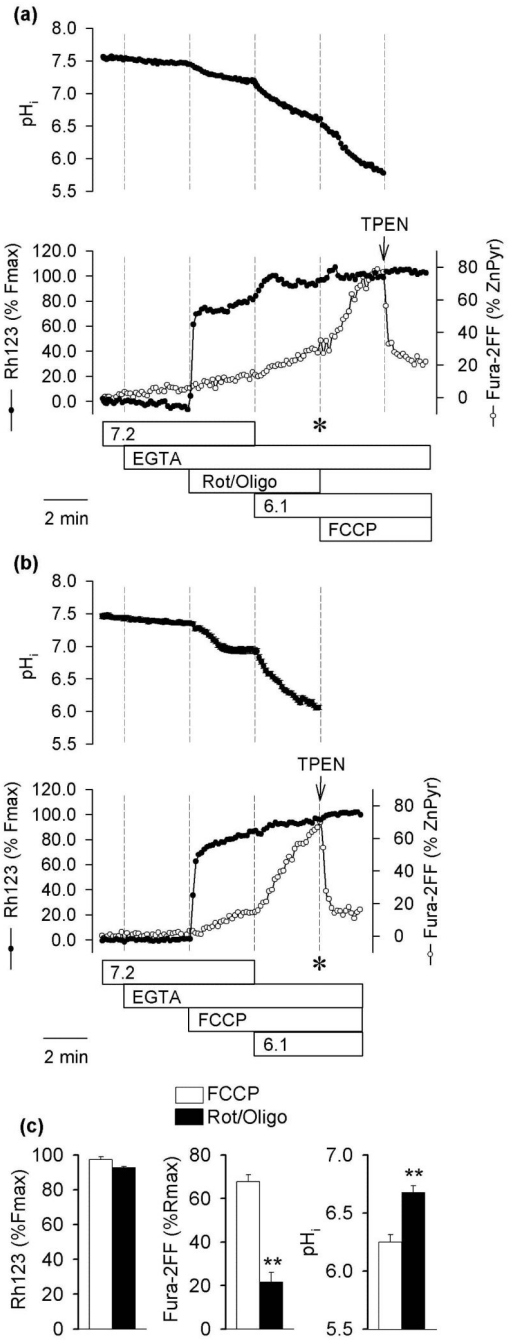


**Fig. 2.**

pH$_i$, Δψm, and $[Zn^{2+}]_i$ in hippocampal neurons exposed to low pH and agents that depolarize mitochondria. (a) Upper panel shows effects of Rot/Oligo (10 μM rotenone plus 5 μg/ml oligomycin) on pH$_i$ monitored using BCECF; lower panel shows effects of Rot/Oligo on Δψm and $[Zn^{2+}]_i$ monitored using Rh123 and Fura-2FF, respectively. Other treatments were the same as described in Fig. 1a. TPEN (10 μM) was applied to determine the extent of $Zn^{2+}$ contribution to the Fura-2FF signal. The data are means from a single experiment on 29 neurons (BCECF) and 24 neurons (Rh123 + Fura-2FF) and represent four to six such

experiments. (b) Experiments analogous to those shown in (a) but FCCP was applied to depolarize mitochondria. The data are means from a single experiment on 28 neurons (BCECF) and 26 neurons (Rh123 + Fura-2FF) and represent four to six such experiments. c) Average $\Delta\psi m$ (Rh123 signal), $[Zn^{2+}]_i$ (Fura-2FF signal), and $pH_i$ measured at the time that is indicated by the asterisks in (a) and (b). The data are means ± SEM from four to six experiments; ** $p<0.01$ Student's t-test.

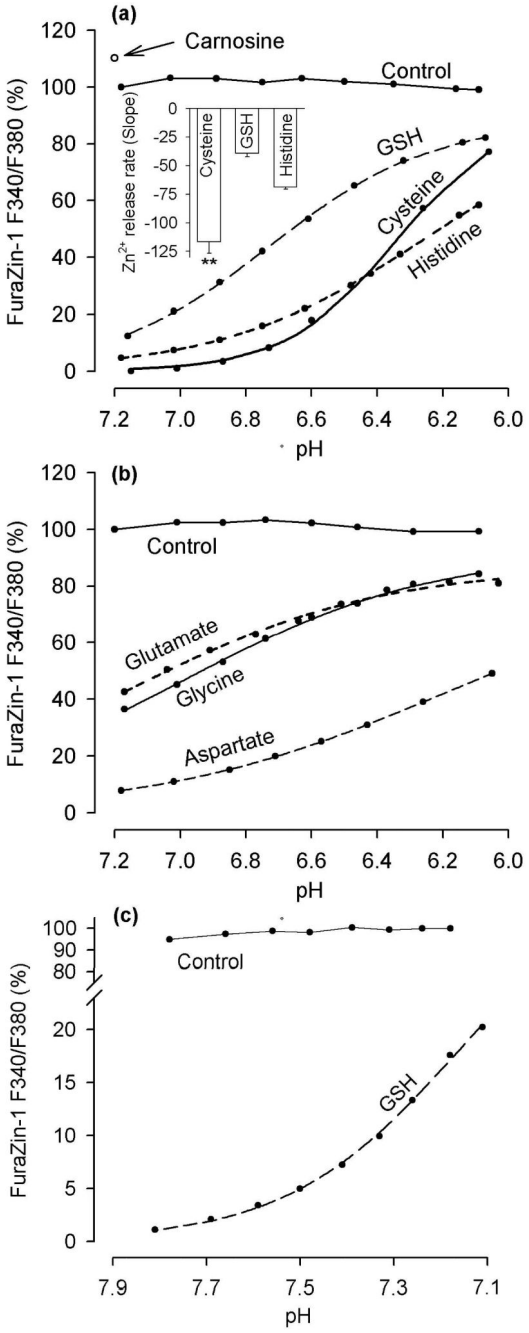


**Fig. 3.**

Effects of pH on $Zn^{2+}$ chelation by tested ligands. (a) Acid-induced $Zn^{2+}$ release from GSH, cysteine, and histidine. The ligands (1 mM) were added to a solution containing 100 nM FuraZin-1, 100 mM KCl, and 50 mM PIPES (37 °C) and the FuraZin-1 signal was measured while pH was manipulated. The inset shows the slopes in the pH range 6.6 - 6.1 (these slopes reflect the rates of $Zn^{2+}$ release from the ligands when pH was decreasing from 6.6 to 6.1); the data are means ± SEM from five to seven experiments identical to those shown in the main figure; ** $p < 0.01$, Cysteine vs GSH, and Cysteine vs Histidine, one way ANOVA

followed by Student-Newman-Keuls test. (b) Acid-induced $Zn^{2+}$ release from glutamate, glycine, and aspartate. The ligands (10 mM) were tested the same way as described in (a). (c) The effect of pH drop from 7.9 to 7.1 on $Zn^{2+}$ chelation by 1 mM GSH. The experiment was performed as described in (a) except that MOPS (instead of PIPES) was used as pH buffer. In all panels, the data are expressed as a percentage of the FuraZin-1 F340/F380 signal measured at pH 7.2 prior to the addition of the ligands; the Control refers to the FuraZin-1 signals measured in the absence of the ligands.

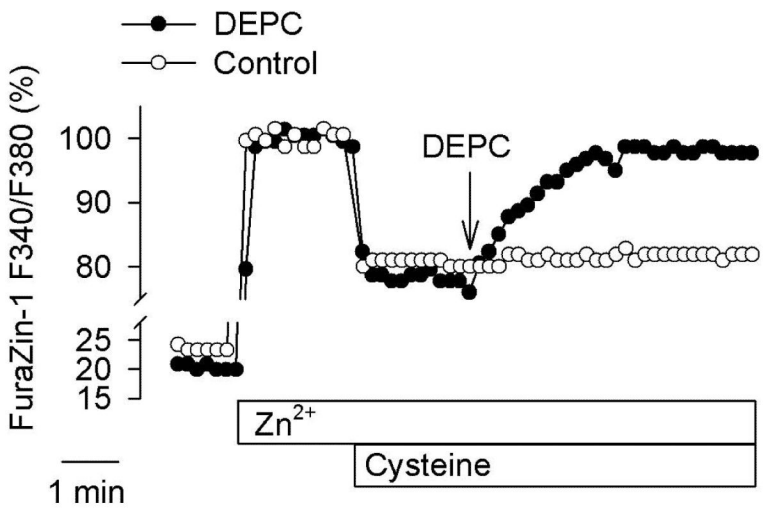


**Fig. 4.**

Diethylpyrocarbonate (DEPC) counteracts $Zn^{2+}$ chelation by cysteine. The F340/F380 ratio was measured *in vitro* in a solution containing 200 nM FuraZin-1, 100 mM KCl, and 50 mM PIPES, pH 7.2. Where indicated, 100 μM $ZnCl_2$, 100 μM cysteine, and 1 mM DEPC were added to the solution; the Control shows data from an experiment without DEPC.